High power 405 nm diode laser fiber-coupled single-mode system with high long-term stability

C. P. Gonschior[a,b], K.-F. Klein[a], D. Heyse[c], S. Baumann[c], T. Sun[b], K. T. V. Grattan[b]
[a]TH Mittelhessen, Wilhelm-Leuschner-Str. 13, 61169 Friedberg, Germany,
e-mail: cornell.p.gonschior@iem.thm.de
[b]City University London, Northampton Square, London EC1V 0HB, United Kingdom,
[c]Omicron-Laserage GmbH, Raiffeisenstr. 5e, 63110 Rodgau, Germany

ABSTRACT

Fiber-coupled 405 nm diode laser systems are rarely used with fiber output powers higher than 50 mW. A quick degradation of fiber-coupled high power modules with wavelengths in the lower range of the visible spectrum is known for several years. Meanwhile, the typical power of single-mode diode lasers around 400 nm is in the order of 100 to 300 mW, leading to single-mode fiber core power densities in the 1 MW/cm² range. This is three magnitudes of order below the known threshold for optical damage. Our profound investigations on the influence of 405 nm laser light irradiation of single-mode fibers found the growth of periodic surface structures in the form of ripples responsible for the power loss. The ripples are found on the proximal and distal fiber end surfaces, negatively impacting power transmission and beam quality, respectively. Important parameters in the generation of the surface structures are power density, surface roughness and polarization direction. A fiber-coupled high-power 405 nm diode laser system with a high long-term stability will be introduced and described.

Keywords: fiber damage, surface damage, ripples, periodic surface structures, UV defects, long-term stability, single-mode laser, single-mode fiber

1. INTRODUCTION

When the output power degradation of 405 nm fiber-coupled diode laser systems was investigated in detail, it became apparent that no photo-degradation or contamination absorbed or attenuated the laser light at this wavelength. The coupling and transmission loss of the laser light was associated to the growth of a laser-induced periodic surface structure (LIPSS) [1]. This LIPSS grows due to the irradiation of the fiber end surface with 405 nm CW laser light and forms a lens and a scattering center on the launching surface (see Figure 1). The additional optical element changes the coupling conditions into the single-mode fiber (SMF). As the structure grows in height, less power is coupled into the fiber core and the fiber output power decreases over time. The main factors contributing to the formation of the LIPSS are the power density, surface roughness, generation of UV defect centers, and the polarization direction of the laser light. The polarization determines the orientation of the ripples, which in our work on silica were found to form parallel to it. This can be confirmed by results from femto-second laser experiments on silica in literature [2]. On the other hand, it was concluded that the other three factors determine the thickness of an unstable ionized surface layer. As shown before, this layer self-organizes into the LIPSS over the period of irradiation [3].

Different end surface preparation methods were compared in earlier work [4]. The application of glass windows is widespread in fiber-coupled high-power laser systems for the near-IR region, especially for fiber laser systems. These so-called end-caps are glass ferrules that are fused to the fiber end, preferably by using CO_2 lasers [5]. The result of using an end-cap is the reduction of power density on the fiber end surface, to mainly prevent mechanical damage of the glass surface. Such a product with silica tubing is also offered commercially [6] and was provided for this work fused to a SMF sample with a CO_2 laser. Through this silica window the laser beam incides with a large spot, the light is then focused into the transmission fiber within the silica material.

During the search for an own solution a possibility was found to splice pieces of multi-mode fiber (MMF) to SMF and cleave the MMF at a precise distance from the splice. Thereby producing a short launch-fiber, like an end-cap, with a good surface quality that can be employed with the SMF inside a standard connector for 125 µm fiber. A patent on the

use of MMF as launch-fiber for small core fibers was already granted in 1987 [7]. In the future the output power of CW diode lasers at 405 nm will increase further and single-mode laser diode modules with 300 mW output power are already commercially available. Therefore, the need for the reduction of power density on a surface with low roughness should be considered for manufacturing a high performance launch-fiber.

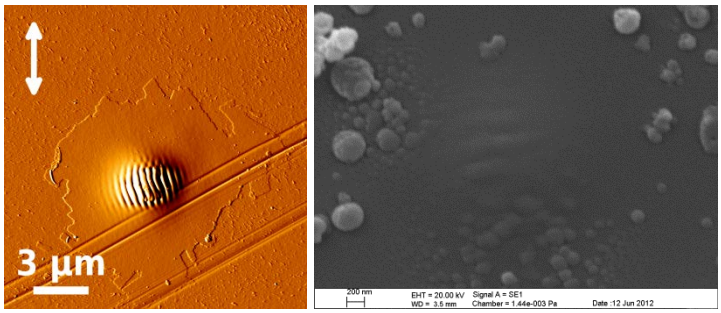

Figure 1: AFM topography gradient of launching SMF end after irradiation with SML without protection on the left (polarization of the laser beam is denoted by the arrow). SEM micrograph of distal SMF end after irradiation with SML without protection on the right (polarization unknown) [1].

Experimental results for improved fiber assemblies will be presented, including the production of assemblies with a high performance launch-fiber. All proximal fiber ends have a launch-fiber. For the investigation of the distal fiber end damage assemblies with and without silica end-cap were prepared. The assemblies were long-term irradiated with 405 nm CW laser diodes. Additionally, a measurement of the beam quality was performed at the fiber output. The results on the distal fiber end damage are compared with step-wise simulations of the growth of a LIPSS on the distal fiber end.

2. EXPERIMENTAL SET-UP

2.1 Measurement set-ups

For the irradiation of the fiber assemblies, a laser diode module (LDM) for 405 nm was used (Omicron-Laserage LDM405.120.CWA.L). This single-mode laser (SML) uses only a single diode, which has a maximum output power of P_{out} = 150 mW. The laser beam is collimated and optically corrected for astigmatism, resulting in a beam quality of M^2 = 1.2. This almost Gaussian beam is suitable for a high coupling efficiency into SMF, which have a slightly better beam quality of M^2 = 1.07. The LDM is current and temperature stabilized for long-term irradiation. The collimated laser beam with a diameter of 1.2 mm is focused on the fiber end surfaces with an imaging and alignment system (IAS) for fibers with FC/PC connectors, which has a focal length of f = 6 mm. The fiber end can be adjusted along the optical axis and tumbled around it. Because of the small spot diameter power densities in the range of MW/cm² are achieved for output powers of a few hundred milliwatts.

The fiber output power $P_{out,fiber}$ from the fibers under test (FUT) was monitored. The FUT were irradiated over a period ranging from eight days to over two months. The loss over time was calculated using:

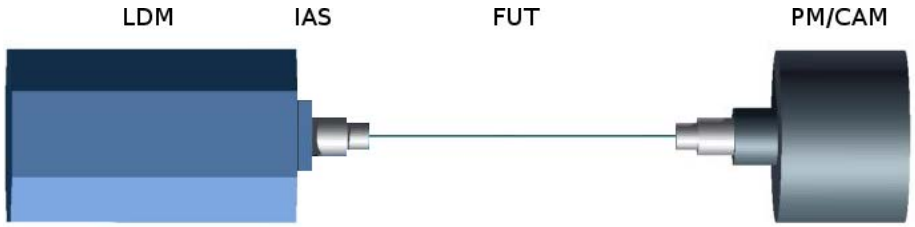

Figure 2: The damage set-up consisting of stabilized laser diode module (LDM) with a wavelength of 405 nm, an imaging and alignment system (IAS) and a thermopile power meter or camera (PM/CAM). The fiber under test (FUT) is aligned for maximal output power.

In all cases the proximal end was adjusted to maximum fiber output power using the IAS. The polarization of the SML was aligned to the slow axis of the polarization-maintaining (PM) fiber. During irradiation, the proximal fiber end was readjusted from time to time to make sure that the system was not misaligned by mechanical or temperature changes. The distal end is in free space and not protected from dust particles. All experiments are conducted in a standard laboratory environment at room temperature. To determine the error in the power reading, the standard deviation of a daily or semi-daily average is added to the uncertainties seen from the power meter and the LDM. For the error of the loss the non-linear propagation of error is used. For the influence of the 405 nm laser radiation on the fiber material the power density I_{core} in the fiber core needs to be taken into account.

For launching light into the fiber end with an attached MMF launch-fiber, it is very important to avoid cutting off too much of the flanks of the Gaussian power distribution. The power P of a Gaussian-shaped beam that is transmitted through an aperture with radius r is given by [9, 10, 11]:

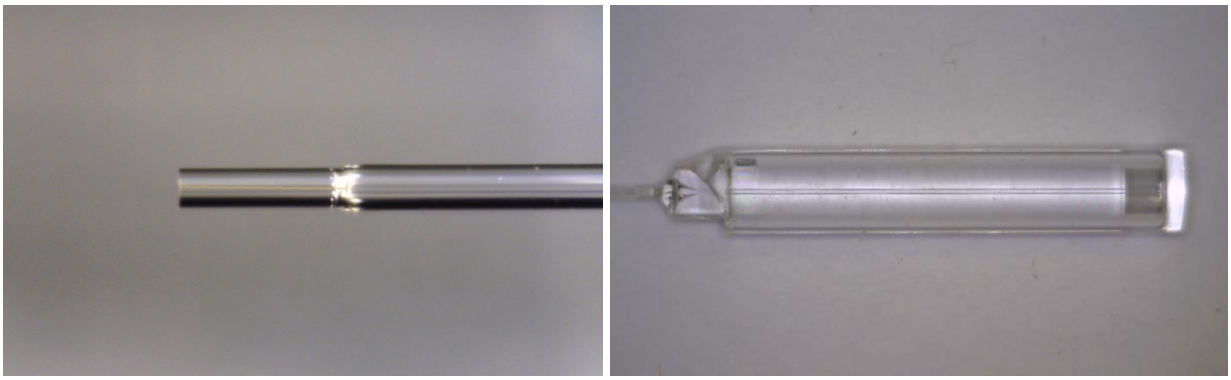

3. RESULTS

3.1 Performance of fiber-coupled diode laser systems with launch fiber

The coupling efficiency from the laser into the SMF through the launch-fiber also depends on the quality of the splice, besides the spot sizes of laser focus and SMF [11]. The light-guiding structure of the SMF could deform in the first few 10 µm due to the heat of the fusion arc. As a consequence the laser light is not guided or coupled with a low loss. Furthermore, the interface between MMF and SMF can get contaminated by burn-off from the electrodes of the fusion arc splicer. In Table 1 the achieved coupling efficiencies for the investigated combinations of *SMF* and *PM-PCF* with launch-fiber of different lengths are reported. The second *SMF* sample with a single launch-fiber was also checked in reverse, with the launch-fiber on the distal end and a bare fiber end on the launching end. In this arrangement the assembly had a fiber output power of 90.7 mW. In comparison to the intended arrangement the coupling efficiency was better, with 65.7 % compared to 47.2 % and 65.1 mW. But with the launch-fiber on the distal end, interference rings were seen in the far field.

Table 1: Coupling efficiencies of transmission systems with *SMF* and *PM-PCF* and launch-fibers of different lengths.

Type	Mode-field diameter [µm]	Length [µm]	$P_{out,fiber}$ [mW]	Coupling efficiency
SMF	2.5	420	53.1 mW	38.5 %
SMF	2.5	450	65.1 mW	47.2 %
PM-PCF	2.6 / 4.3 (elliptical)	490	72.2 mW	52.3 %

The fiber output power $P_{out,fiber}$ was stabilized to a large degree in the samples with launch-fiber. Figure 4 shows that the damage rate is below 0.03 dB/day for the protected samples. For comparison, the damage rate for *SMF* samples without protection irradiated with the SML was 0.2 to 1 dB/day, depending on the surface preparation [4]. On the surfaces of the launch-fiber no damage could be found after the irradiation. The first assemblies had a low coupling efficiency. Nevertheless, power densities I_{core} in the SMF cores of 800 kW/cm² to 1.3 MW/cm² were reached.

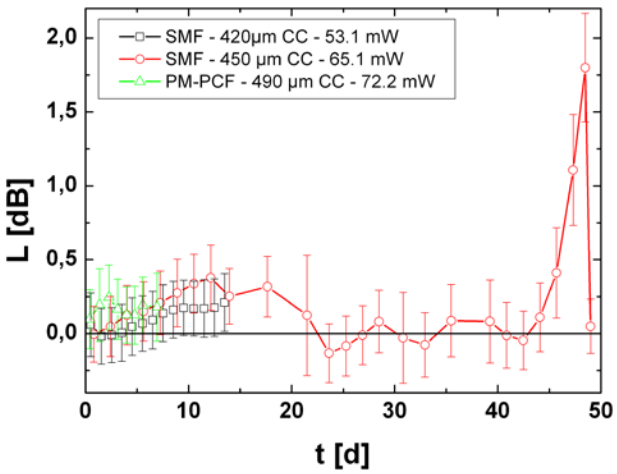

Figure 4: Loss over time of *SMF* and *PM-PCF* samples with launch-fiber irradiated with the SML. The second sample (red circle) was adjusted several times during irradiation. The given power is the fiber output power at the beginning of the measurement.

When the second assembly with *SMF* (red circle in Figure 4) showed a higher loss of 0.38 dB after 14 days, the distal end was cleaved off. The loss was thereby reduced by 0.13 dB. It was noticed that the divergence angle of the beam coming from the fiber was smaller after the damaged distal end was cleaved off. Therefore it was assumed that the reduction in power that was measured was not due to a loss, but due to an increase in far-field angle. The light spot was larger than the aperture of the power meter and could not be completely collected. The distal end was then repeatedly cleaved off to achieve constant power measurement over the course of irradiation. The last of seven cleaved surfaces showed the lowest measured power after 12 days of irradiation, but when it was cleaved off all the light could be collected again for the power measurement. For this last sample of damaged end surfaces an M^2 measurement was performed directly after cleaving and after the 12 days of irradiation. On one axis a degradation from $M^2 = 1.2 \pm 0.2$ to $M^2 = 5 \pm 0.5$ was measured and on the axis perpendicular to that a degradation from $M^2 = 1.6 \pm 0.2$ to $M^2 = 9 \pm 0.5$.

The increase in far-field angle of the light emitted from the fiber end was most notable for the assembly with *PM-PCF*. Before the irradiation the web around the PCF core was also illuminated and projected onto the screen, shown in Figure 5 a). This projection of the web got more blurry over the course of irradiation, until after five days in Figure 5 c) mainly the core was projected onto the screen. At the same time the increase in divergence angle was obvious, but constrained to the vertical axis.

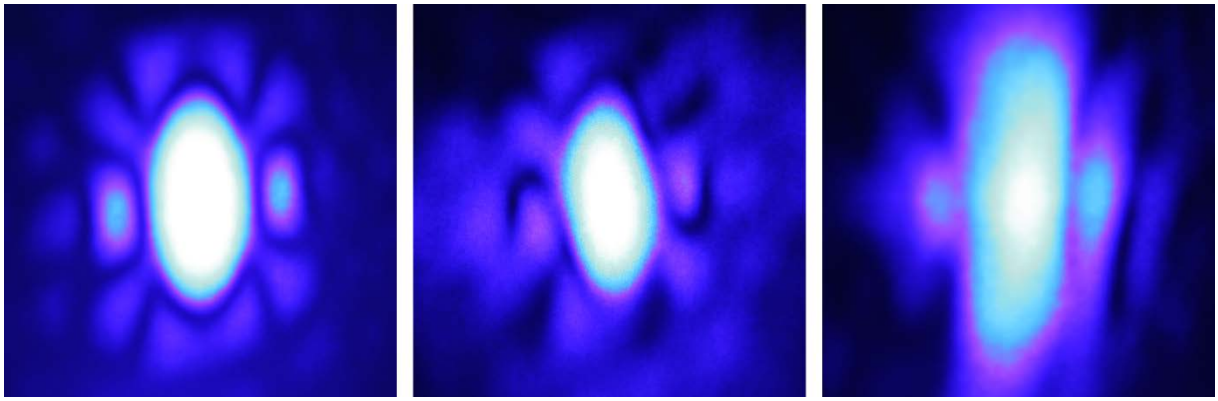

a) b) c)

Figure 5: Photographs of the far-field of the *PM-PCF* assembly on a screen for a) the pristine end surface, b) irradiated for one day and c) irradiated for five days.

3.2 Performance of fiber-coupled diode laser system with launch fiber and silica end-cap

In Table 2 the achieved coupling efficiency for the investigated combination of *PM-SMF* with launch-fiber on the proximal and a silica end-cap on the distal end is reported. The *PM-SMF* assembly was irradiated with the SML and the longest irradiation experiments were performed on this particular assembly. A very slow linear degradation of 0.01 dB/day is visible in Figure 6 for the first 35 days. After an inspection of the freely accessible end-cap with an optical microscope and with a white screen in the far field the issue could be resolved (see Figure 7). Over the long irradiation period dust particles had accumulated in the area where the beam passed through the silica-air interface. The dust particles scattered the light which then could not be collected by the power meter completely. The end-cap could be easily cleaned by wiping off the dust. The far-field image showed a clean Gaussian distribution again and the power meter could collect more power. However, the loss could only be improved by 0.35 dB. After the cleaning process the slow degradation commenced.

When the experiment was discontinued after 60 days, the surface of the launch-fiber on the *PM-SMF* was inspected, too. It showed an accumulation of contamination across the whole surface. This contamination was also easily removable by using optics cleaning wipes. In a parallel experiment the launch-fiber was observed to be completely clean after irradiation.

Table 2: Coupling efficiency of transmission system with *PM-SMF*, launch-fiber and silica end-cap on the distal end.

Type	Mode-field diameter [µm]	Length [µm]	$P_{out,fiber}$ [mW]	Coupling efficiency
PM-SMF	3.2	530	81.2 mW	58.8 %

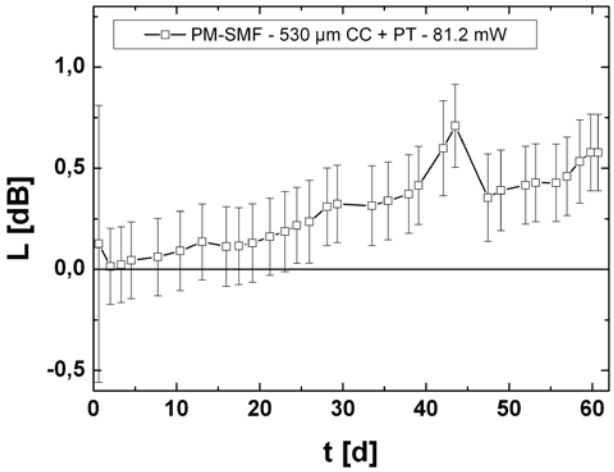

Figure 6: Loss over time of the *PM-SMF* sample with launch-fiber and end-cap irradiated with the SML. The sample was adjusted several times during irradiation. The given power is the fiber output power at the beginning of the measurement.

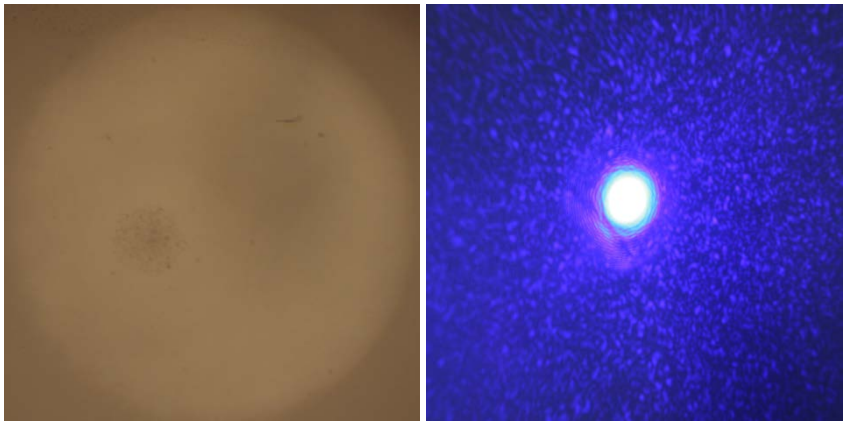

Figure 7: Picture of silica end-cap on *PM-SMF* after 44 days of irradiation on the left. Picture of far field emitted from contaminated silica end-cap on *PM-SMF* on the right.

4. SIMULATION OF DISTAL END SURFACE DAMAGE

The influence of a growing surface structure on the beam quality at the distal end was reconstructed using simulations. The software that was employed uses the finite-difference time-domain method and is called FDTD Solutions (Lumerical Solutions, Inc.). A SMF with a core radius of a = 1.2 µm, a refractive index of n_{Co} = 1.45441 (SiO_2 glass at 405 nm, [12]) in the core and of n_{Cl} = 1.44956 (F doped SiO_2) in the cladding was designed, giving a numerical aperture of 0.12 and a V number of 2.2 at λ_0 = 405 nm. The cut-off wavelength for this SMF is 376 nm. These values are in good

correspondence to the specifications of the *SMF*. As a light source the fundamental mode with λ_0 = 405 nm was excited in the fiber core, which is easily possible with the simulation tool.

The surface structure was also modeled out of SiO_2 glass with a diameter of 3 µm and eleven sinusoidal ripples across, which is a periodicity of about Λ = 273 nm. Additional parameters for the growth of the structure, like height in the center, the radius of curvature, and the amplitude of the ripple, are given in Table 3. The periodic structure was designed to fit the surface structure measured with AFM on a launching surface of a SMF [4]. The smaller periodic structures are down scaled designs of the 700 nm high structure. After the actual form of LIPSS on pre-irradiated cores were found with SEM analyses, an additional structure was modeled with a diameter of 2 µm and almost no lens property or more specifically with high ripple amplitude. Seven sinusoidal ripples across the 2 µm result in Λ = 285 nm.

Table 3: Parameters and determined properties of simulated surface structures.

Height [nm]	**Radius of curvature [µm]**	**Ripple amplitude [nm]**	**Focal length [µm]**	**w_0 [µm]**	**z_R [µm]**
0	N/A	N/A	N/A	1.3	12.25
100	11	15	5.3	1.08	8.46
300	3.6	40	4.2	0.67	3.25
500	2.2	70	3.3	0.465	1.57
700	1.5	100	2.6	0.33	0.79
700 (no lens)	0.7	500	∥ 1.3; ⊥ 1.3	∥ 0.31; ⊥ 0.29	∥ 0,697; ⊥ 0,61

Examples of the power distribution of light excited inside the SMF and transmitted through the LIPSS is shown in Figure 8. The SMF light source has a length of 3 µm after which the LIPSS is positioned. In the case without LIPSS the light propagation is according to the Gaussian beam equations (a). In case of the 700 nm high LIPSS with lens property the light is strongly focused behind the end surface (b). The result for the LIPSS without lens property and smaller diameter also exhibits the focusing effect. This is shown in Figure 8 c) for the power distribution perpendicular to the orientation of the ripples. The focal length *f* and spot size w_0 can be determined at the point of highest intensity.

If a LIPSS forms a lens and a scattering center on the distal end of the fiber its major impact is on the divergence angle of the emitted light. If the light is collected with a detector with an aperture radius of *r*, then the detected power P_{det} is described by Formula 6. The beam radius *w(z)* and the Rayleigh length z_R are calculated according to Formulae 7 and 8, with $n = 1$ and $M^2 = 1.07$ for a SMF. The beam spot size w_0 depends on the LIPSS that was simulated and was determined in the focus behind the fiber end. For a distal fiber end without a structure the spot size of the fiber was determined. The Rayleigh lengths and the spot sizes received from the experiments are shown in Table 3.

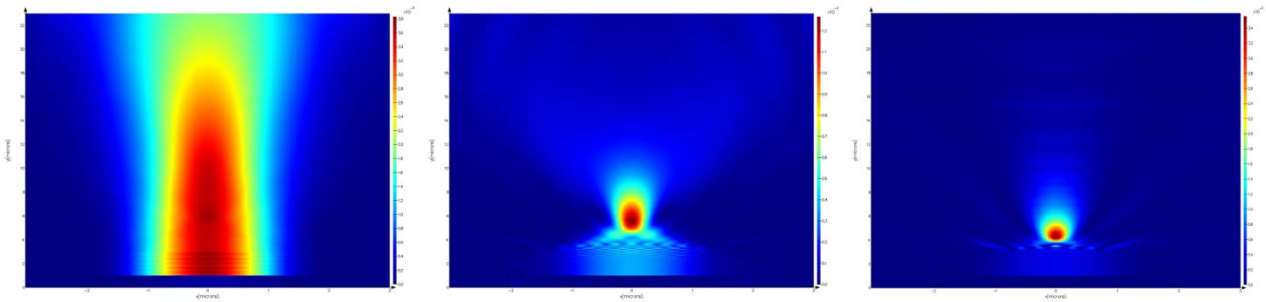

a) b) c)

Figure 8: Power distributions of light transmitted from SMF a) without LIPSS, b) through 700 nm high LIPSS, c) through 700 nm high LIPSS without lens property perpendicular to orientation of the ripples. The graphs exhibit some interferences from reflections at the boundary conditions.

A simple aperture test, with the power detector as aperture (r = 9.5 mm), was performed before and immediately after cleaving off the last distal end of the second *SMF* sample. The detector is located 17 mm inside the power meter housing. The power meter was being moved away from the fiber and measurements of P_{det} were taken at distances z of 17, 22, 27, 32, 37, 77 and 102 mm between fiber surface and detector plane. The loss $L_{det}(z)$ due to less detected power with a movable aperture in z direction is shown in Figure 9. For the case without a surface structure, simulation and measurement are in very good agreement. The distal end that was damaged for 12 days had an unknown height and a base diameter of 2 µm, which is smaller than the fiber mode-field diameter. The simulation of a LIPSS with 3 µm in diameter might not be very appropriate, but the measured loss curve after 12 days falls well onto the LIPSS with a height of 700 nm. A comparison with the loss curves of the LIPSS with the smaller diameter of 2 µm and without lens property reveals a similar behavior. The loss at z = 27 mm (10 mm distance between power meter and fiber) is the same as the maximum in Figure 4, because this was the standard distance in the long-term experiments.

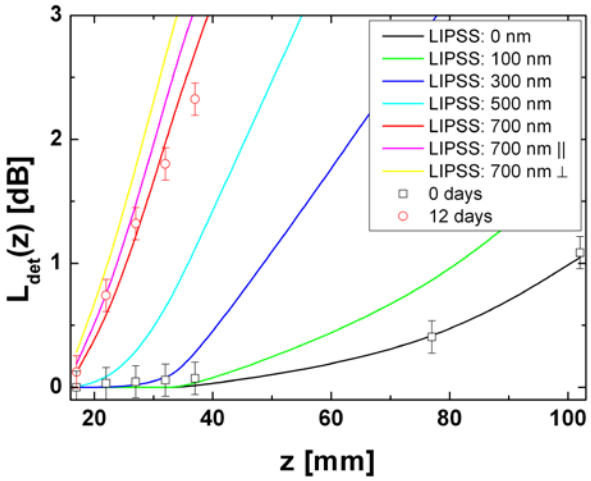

Figure 9: Loss due to less detected power along z, the distance from the fiber end surface, for a detector radius of 9.5 mm. The lines represent the simulation results for different heights of LIPSS. The symbols are the measurements at specific distances from the fiber end surface for an undamaged surface and a surface exposed for 12 days.

5. DISCUSSION

The propagation of a beam into a launch-fiber or silica end-cap can be completely described using Gaussian beam and far-field equations. The optimal length for a high performance concerning surface damage was found to be in the range of 500 µm for the laser system used in this work. The prepared samples had lengths of the launch-fiber between 420 µm and 530 µm. In all cases a fiber output power of 50 mW was achieved and for the best samples the coupling efficiency was above 50 %.

The loss in fiber output power that was measured in some cases cannot be attributed to an actual transmission loss. When a laser-induced periodic surface structure (LIPSS) forms on the distal end surface, the light is scattered and focused with a very short focal length. This in turn degrades the beam quality and increases the far-field angle. Since the detected power was just a part of the fiber output power for higher far-field angles, Formula 1 needs to use P_{det} instead of $P_{out,fiber}$. This was also proven by the simulations of a LIPSS on a distal fiber end. The detected power decreases at a constant distance from the fiber surface due to an increasing far-field angle. Thereby, the transmitted power $P_{out.fiber}$ is proven to have been constant.

The most stable fiber system was found to have a launch-fiber on the proximal end, for ease of assembling with a connector, and a silica end-cap on the distal end. Thus, both silica-air interfaces were protected from high power densities. The launch-fiber was prepared from a MMF with low solarization and by using improved surface roughness.

These improvements should show their effect for extremely long-term irradiation or very high laser power. The two systems that were examined had a high output power with good coupling efficiencies of about 60 and 75 %. The only degradation of the measured power that was found was an accumulation of dust particles on the silica-air interface. Those are attracted by the lightly ionised surface and can be easily wiped off. A high stability of the systems with a loss rate of only 0.01 dB/day and no damage on either end promises high performance for long-term use in high-power applications.

6. CONCLUSIONS

An improvement in the damage behavior of SMF in fiber-coupled 405 nm diode laser systems was achieved by specifically implementing conditions which take the influential parameters into account. The major advance was the reduction of the power density on the fiber launching end. For that purpose a short cleaved launch-fiber was produced. As a preparation for future higher power laser diodes, the launch-fiber was made from a very low solarization multi-mode fiber. The damage on the distal fiber end was characterized by M^2 measurements and aperture tests. Simulations showed the negative impact of the damage on the beam quality. In order to prevent this damage, a silica end-cap was used on the distal end. This assembly performed with high stability over a period of two month of constant irradiation with the 405 nm single-mode laser.

7. ACKNOWLEDGEMENTS

We would like to acknowledge support from the German Federal Ministry of Education and Research through AiF under grant FKZ 1737X08.

REFERENCES

[1] Gonschior, C. P., Klein, K., Sun, T. and Grattan, K. T. V., “Generation of periodic surface structures on silica fibre surfaces using 405 nm CW diode lasers”, Journal of Non-Crystalline Solids 361: 106-110 (2013).
[2] Hoehm, S., Rosenfeld, A., Krueger, J. and Bonse, J., “Femtosecond laser-induced periodic surface structures on silica”, Journal of Applied Physics 112: 014901 (2012).
[3] Reif, J., Costache, F. and Bestehorn, M., “Self-Organized Surface Nanostructuring by Femtosecond Laser Processing”, [Recent advances in laser processing of materials], Perrière, J., Millon, E. and Fogarassy, E. (Eds.), Elsevier, 275-290 (2006).
[4] Gonschior, C. P., Klein, K., Sun, T. and Grattan, K. T. V., “Influence of high power 405-nm multi-mode and single-mode diode laser light on the long-term stability of fused silica fibers”, Proc. SPIE 8426, 24 (2012).
[5] Boehme, S., Beckert, E., Eberhardt, R. and Tuennermann, A., “Laser splicing of end caps: process requirements in high power laser applications”, Proc. SPIE 7202, 05 (2009).
[6] Acuna, R., and Zhou, J., “Innovative patent-pending end cap for high power laser-fiber coupling”, Laser Focus World 46 (2010).
[7] Emkey, W. L. and Jack, C. A., “Multimode fiber-lens optical coupler”, Patent US4701011 (1987).
[8] Paschotta, R., [Encyclopedia of Laser Physics and Technology], Wiley-VCH, Berlin (2008).
[9] Sun, H., [Laser diode beam basics, manipulations and characterizations], Springer (2012).
[10] Marcuse, D., [Light transmission optics], Van Nostrand Reinhold (1982).
[11] Neumann, E., [Single-mode fibers: Fundamentals], Tamir, T., (Ed.), Springer (1988).
[12] Palik, E. D., [Handbook of Optical Constants of Solids], Elsevier (1997).